Published in final edited form as:
J Nucl Med. 2012 June ; 53(6): 841–844. doi:10.2967/jnumed.111.099853.

Advances in Preclinical SPECT Instrumentation

Todd E. Peterson[1,2,3] and **Sepideh Shokouhi**[1,2]

[1]Institute of Imaging Science, Vanderbilt University, Nashville, Tennessee

[2]Department of Radiology & Radiological Sciences, Vanderbilt University, Nashville, Tennessee

[3]Department of Physics & Astronomy, Vanderbilt University, Nashville, Tennessee

Abstract

Preclinical SPECT imaging of rodents is both in demand and very demanding. The need for high spatial resolution in combination with good sensitivity has given rise to considerable innovation in the areas of detectors, collimation, acquisition geometry, and image reconstruction. Some of the developments described herein are beginning to carry over into clinical imaging as well.

Keywords

SPECT; preclinical imaging; semiconductor detectors; multi-pinhole collimation; synthetic collimator

Preclinical imaging of small animals plays an important role not only in the development of new imaging agents, but also in biological studies of both disease and non-disease states as well as in drug development. While *in vivo* preclinical studies pave the way for new clinical applications of molecular imaging, they also provide an important testing ground for new instrumentation and image-acquisition strategies that themselves have the potential to transform clinical molecular imaging. The focus of this article will be on innovation in preclinical SPECT, although other modalities have seen similar developments. To image organs or structures within a mouse with a similar quality as that of a human requires improvements in both spatial resolution and sensitivity over clinical SPECT. Attempting to meet the sensitivity-resolution demands of preclinical SPECT has led to innovation in collimation, detectors, calibration, and image reconstruction. In this brief article we will survey these developments through the lens of our own research efforts.

Collimation

Multi-pinhole collimation has become the standard approach in most preclinical SPECT systems because of the ability to obtain good spatial resolution through pinhole magnification while enhancing sensitivity though the incorporation of multiple pinholes. In the standard formulation, the planar spatial resolution of a pinhole is

$$R_{total} = \sqrt{d^2\left(1+\frac{1}{M}\right)^2 + R_{det}^2 / M^2} \quad (1)$$

Corresponding Author: Todd E. Peterson, Ph.D., Vanderbilt University Institute of Imaging Sciences (VUIIS), Vanderbilt University Medical School, 1161 21st Ave. S., AA 1105 MCN, Nashville, TN 37232-2310; Tel: (615) 322-2648; Fax: (615) 322-0734; todd.e.peterson@vanderbilt.edu.

where d is the pinhole diameter, M is the magnification, and R_{det} is the intrinsic detector resolution; while the sensitivity to a point source (fraction of emitted photons passing through the pinhole) is given by

$$S = \frac{d^2}{16h^2} cos^3\theta, \quad (2)$$

where h is the perpendicular distance from the pinhole, and θ is the angle between the point-to-pinhole projection line and the normal to the detector. The sensitivity-resolution tradeoff for pinhole collimation is immediately apparent. While the spatial resolution scales approximately linearly with pinhole diameter, the sensitivity is proportional to the square of the pinhole diameter; shrinking the pinhole diameter to improve the spatial resolution comes with a steep penalty in sensitivity.

These simplified equations ignore several effects, such as details of pinhole geometry and photon penetration at pinhole edges. Depending on the collimator design, acquisition geometry, and photon energy, these effects can become sufficiently large so that their inclusion is necessary to accurately model pinhole projections. The amount of pinhole penetration depends on the photon energy and collimator material and represents a limiting factor in spatial resolution. Iodine-125-labelled radiotracers are sometimes used in preclinical SPECT, and their low photon energy limits pinhole penetration, reducing the effective pinhole diameter and enabling better resolution relative to higher energy radionuclides. The geometric sensitivity in equation 2 does not explicitly include the pinhole opening angle, shape, or thickness. Deviation from this expression has been shown to occur when using small pinhole opening angles, which reduce penetration, and short object-to-collimator distances, which improve sensitivity and resolution (1), and it can be important to consider such effects when designing new systems.

Increasing the number of pinholes in a collimator can either improve the sensitivity and angular sampling for a fixed field of view or else enlarge the field of view, depending on how the pinhole positions and focal points are chosen. The primary limitation in multi-pinhole collimator design is the overlap of the projections from different pinholes. This so-called multiplexing creates ambiguity as to which pinhole a detected photon may have passed through, reducing the sensitivity advantage of the added pinholes and possibly leading to artifacts in the reconstructed images. The amount of multiplexing and its effect on image reconstruction has been the subject of some studies on multi-pinhole collimator design (2, 3). While some preclinical scanners, such as the U-SPECT system from MILabs (4), employ multi-pinhole collimation with conventional gamma cameras with no multiplexing to avoid any potential problems, the Bioscan NanoSPECT delivers high-quality images despite allowing some multiplexing of projections (5). Rentmeester et al (6) investigated the optimal multi-pinhole SPECT configuration when no multiplexing is allowed, but the larger parameter space created when multiplexing is allowed makes for a daunting optimization problem. In simulation studies in which only the number of pinholes in a fixed geometric configuration were varied, Cao et al found that a camera with a nine-pinhole collimator gave the best performance for their quantitative mouse brain-imaging task (7). Importantly, changes in the geometric configuration of the pinholes would likely change the outcome, due to differences in angular sampling and multiplexing, while Mok et al demonstrated that the performance of a multiplexed multi-pinhole system also depends on the object activity distribution (3).

Our approach to increasing sensitivity through the use of multi-pinhole collimation has been to allow multiplexing, but to acquire data in such a way that it contains information about

the multiplexing. This approach is known as synthetic collimation and involves the acquisition of pinhole projection data at multiple magnifications (Figure 1) (8, 9). The basic concept behind the synthetic-collimator approach is to combine lower-resolution data containing little (or no) multiplexing with higher-resolution data that is more highly multiplexed. The lower magnification data then contains information about the nature of the multiplexing in the higher magnification data such that, when combined in an appropriate image reconstruction algorithm, SPECT images largely free of artifacts can be generated. How best to choose the pinhole overlap and magnifications is the subject of ongoing investigations (9).

Detectors

The advancement of new imaging detector approaches has been driven in part by the demand for improved small-animal imaging capabilities. Despite some differences, all multi-pinhole collimation approaches can benefit from higher intrinsic detector resolution. As can be seen from equation 1, improvements in detector resolution lower the magnification required for a desired image resolution, allowing for either reductions in multiplexing for a given pinhole configuration or an increase in the number of pinholes. Alternatively, the reduced area needed to accommodate the projection through a single pinhole means smaller detectors can be used. These considerations have led investigators to explore alternatives to conventional gamma cameras. Beyond the practical appeal of more compact systems, this aspect means that it is possible to explore new detector technologies that may be expensive or difficult to create in large format or number. We can provide here only a brief summary of some of these approaches. For greater detail, the interested reader is referred to the recent review article on SPECT detectors (10).

Just as in clinical SPECT, continuous scintillator crystals read out with multiple photomultiplier tubes play an important role in preclinical SPECT. While position estimation based on Anger logic continues to be used, increased computational power has enabled practical implementation of maximum-likelihood estimation, offering improvements in performance for continuous-crystal detectors (11). Alternatively, gamma cameras based on pixellated arrays of scintillator crystals can provide spatial resolution of around one millimeter through the confinement of the scintillation light to an individual crystal within the array. Besides the practical difficulties of assembling an array with crystals of ever smaller dimensions, attempts to achieve better spatial resolution through the use of smaller crystals are faced with reduced detection efficiency due to the unavoidable gaps between crystals, as well as degradation in energy resolution from poor light collection efficiency. Since the position estimation also depends on generating sufficiently large signals to distinguish one crystal from another, a balance must be found between the size of the crystals and the ability to reliably identify in which crystal an interaction occurred.

Another scintillator-based approach is to utilize a CCD or CMOS device to collect the scintillation light, with several different means of transmitting the scintillation light from crystal to CCD having been used, including fiber-optic tapers and lenses. Detector systems of this type have demonstrated intrinsic spatial resolution of less than 100 micrometers (12-14). The energy resolution in such approaches tends to be relatively poor, and often the outstanding spatial resolution is achieved by using thin scintillators, requiring a sacrifice in detection efficiency.

Semiconductor detectors also have received considerable attention for preclinical SPECT due to their outstanding energy resolution and ability to provide good spatial resolution via highly segmented readout electrodes. While most of the effort for SPECT applications has focused on CdZnTe, with CdTe also receiving considerable attention, our own efforts have

focused on two other semiconductors, silicon and germanium, that offer some interesting advantages along with some challenges. While high degrees of detector segmentation are possible, the chief drawback is the increase in readout channels required as detector electrodes shrink in size. The silicon detectors that we use, shown in figure 2A, utilize a double-sided strip configuration, with the electrodes on the front and back divided into strips that are laid out orthogonally on the two sides. Photon interaction position is estimated in two dimensions by the intersection of the front and back strips on which charge is collected. This enables reporting of N^2 positions by reading out only $2N$ strips. The silicon detectors with which we have been working are one-millimeter thick and consist of 1024 × 1024 strips at a pitch of 59 micrometers, effectively providing an intrinsic resolution of 59 μm (figure 2B) (11). Two additional features make them ideal for the synthetic-collimator imaging. First, the double-sided strip format means that the electrical connections and associated readout electronics can be located to the outside of the detector, enabling mounting in a transmission configuration. The second key feature is the modest detection efficiency of silicon in the 30-keV energy range. While the ~30% absorption of Iodine-125 photons in one millimeter of silicon seems less than desirable, the fact that ~70% proceed through the detector unaffected, taken along with the transmission configuration, means that silicon detectors can be stacked one behind the other. This stacking increases the total detection efficiency and enables multi-pinhole projection data to be acquired at multiple magnifications simultaneously.

More recently, we have begun investigating the potential of germanium double-sided strip detectors for small-animal SPECT. While the excellent energy resolution has long made it an appealing material for SPECT owing to the possibility of effective scatter rejection and multi-isotope imaging, segmentation of electrodes on germanium is difficult compared to other semiconductors and the requirement of operation at liquid-nitrogen temperatures has been seen as undesirable. Recent technological advances have given rise to compact double-sided strip detector systems utilizing mechanical cooling, rendering liquid nitrogen dewars unnecessary (figures 2C & 2D). The outstanding charge collection that enables such good energy resolution also facilitates the use of position-estimation techniques to achieve sub-strip spatial resolution along with estimation of the depth of interaction. The depth determination is based on the rise-time differences between the signals on the front and back sides, while the lateral positioning can be estimated from the ratio of the fast transient signals induced on the neighboring strips as charges drift toward the charge-collecting strip. Using this approach we have been able to demonstrate intrinsic resolution of better than 1.5 mm in all three dimensions, while also achieving less than 1% FWHM energy resolution at 140 keV with a detector consisting of 16 × 16 strips at a pitch of five millimeters on a crystal that is one-centimeter thick and nine centimeters in diameter (15). Some sense of the potential of this detector technology for multi-isotope imaging can be inferred from the pulse-height spectrum shown in Figure 3.

Acquisition Geometry

SPECT acquisition generally involves the rotation of a single or multiple camera heads in a circular orbit. Sometimes helical orbits are employed to improve the angular sampling completeness at short distances (16). Stationary multi-pinhole SPECT is desirable because it eliminates motion-related errors, reduces geometry-related calibration errors, and enables dynamic imaging. One difficulty in stationary SPECT is that limited angular sampling in compact systems can result in streak artifacts and geometric distortion. The FastSPECT II system successfully employs a full-ring stationary configuration (17), while the U-SPECT systems use stationary cameras with linear translation of the subject to improve sampling (4). Our studies have shown that with the synthetic-collimator approach high-angular

sampling completeness can be achieved in a mouse-brain-sized FOV using only two stationary camera heads in an orthogonal geometry (9).

Calibration & Reconstruction

Efforts to provide the needed spatial resolution and sensitivity for preclinical SPECT have placed new demands on both system calibration and image reconstruction algorithms. The issues and methods to address them are clearly described in (18). Iterative statistical algorithms (19) are the standard approach for image reconstruction in preclinical SPECT. Iterative algorithms utilize a model of the imaging system to forward-project an object estimate, compare it to experimental projection data, and iteratively update the estimate of the object distribution. They allow for accurate accounting of pinhole geometry and photon penetration effects. Furthermore, iterative methods can include realistic models of detector resolution by either including the depth-of-interaction blurring or, alternatively, including the depth-of-interaction information from detectors that have such capabilities. On the calibration front, achieving sub-millimeter resolution requires precise knowledge of the relative locations of the pinholes and detectors. In systems utilizing rotating cameras, it has been found necessary to account for mechanical deviations in the camera orbits that are of negligible importance in clinical SPECT due to the substantially poorer spatial resolution (20).

The most accurate, yet tedious, way to obtain the system model is to directly measure it by stepping a point source through the field of view, thereby fully accounting for the geometry as well as collimator and detector responses. Similarly, this can be done within reasonable approximation through a Monte Carlo simulation, eliminating practical difficulties related to experimental measurements. With either method the need for sufficient statistical quality in the system model requires lengthy acquisition/simulation time. One can also calculate the system model by using analytical models for collimator sensitivity and detector response. Despite limitations, this approach is essential for design studies, where a wide range of system parameters and their impact on image quality need to be systematically investigated.

Attenuation and scatter are not as significant in small-animal SPECT as clinical, and therefore are often neglected in image reconstruction. It has been shown that performing attenuation correction without scatter correction can lead to a significant overestimation of activity concentration, but that high quantitative accuracy can be achieved by correcting for both effects (21, 22). Partial volume errors also can lead to significant underestimation of activity concentration in many small-animal SPECT scenarios, providing impetus to improve resolution through smaller pinholes, higher magnification, and/or better detector resolution. However, if gains in resolution come at too large of a cost in sensitivity, then the improvement in quantitative accuracy can be accompanied by a decrease in precision due to greater noise.

Conclusion

The demand for preclinical SPECT capabilities, as well as the demands placed on the instrumentation to create useful preclinical SPECT images, has led to considerable innovation. Quantitative images can now be obtained with sub-millimeter spatial resolution at a practical sensitivity. Furthermore, some of the technologies first demonstrated in preclinical SPECT are beginning to find use in clinical imaging. CdZnTe detectors can now be found in dedicated cardiac SPECT systems (23, 24), while both CdZnTe detectors and pixellated scintillators are used for breast imaging (25, 26). Multi-pinhole approaches are under investigation for brain imaging (27) and have been employed in a static, limited-angle configuration for cardiac imaging (24).

Acknowledgments

This work was supported in part by NIH grants R33EB00776, R01EB013677, K99EB009106 and Department of Energy grant DE-SC0002437. We gratefully acknowledge the important contributions of Desmond L Campbell, Heather L Durko, Lindsay C Johnson, Benjamin S McDonald, and Oleg Ovchinnikov to the silicon and germanium detector work.

Financial Support: NIH grants R33EB00776, R01EB013677, K99EB009106 and Department of Energy grant DE-SC0002437

References

1. Shokouhi S, Metzler SD, Wilson DW, Peterson TE. Multi-pinhole collimator design for small-object imaging with SiliSPECT: a high-resolution SPECT. Phys Med Biol. 2009; 54:207–225. [PubMed: 19088387]
2. Vunckx K, Suetens P, Nuyts J. Effect of overlapping projections on reconstruction image quality in multipinhole SPECT. IEEE Trans Med Imaging. 2008; 27:972–983. [PubMed: 18599402]
3. Mok GS, Tsui BM, Beekman FJ. The effects of object activity distribution on multiplexing multi-pinhole SPECT. Phys Med Biol. 2011; 56:2635–2650. [PubMed: 21454926]
4. Vastenhouw B, Beekman F. Submillimeter total-body murine imaging with U-SPECT-I. J Nucl Med. 2007; 48:487–493. [PubMed: 17332628]
5. Schramm NU, Ebel G, Engeland U, Schurrat T, Behe M, Behr TM. High-resolution SPECT using multipinhole collimation. IEEE Trans Nucl Sci. 2003; 50:315–320.
6. Rentmeester MC, van der Have F, Beekman FJ. Optimizing multi-pinhole SPECT geometries using an analytical model. Phys Med Biol. 2007; 52:2567–2581. [PubMed: 17440253]
7. Cao Z, Bal G, Accorsi R, Acton PD. Optimal number of pinholes in multi-pinhole SPECT for mouse brain imaging--a simulation study. Phys Med Biol. 2005; 50:4609–4624. [PubMed: 16177493]
8. Wilson DW, Barrett HH, Clarkson EW. Reconstruction of two- and three-dimensional images from synthetic-collimator data. IEEE Trans Med Imaging. 2000; 19:412–422. [PubMed: 11021685]
9. Shokouhi S, Wilson DW, Metzler SD, Peterson TE. Evaluation of image reconstruction for mouse brain imaging with synthetic collimation from highly multiplexed SiliSPECT projections. Phys Med Biol. 2010; 55:5151–5168. [PubMed: 20714046]
10. Peterson TE, Furenlid LR. SPECT detectors: the Anger camera and beyond. Phys Med Biol. 2011; 56:R145. [PubMed: 21828904]
11. Barrett HH, Hunter WCJ, Miller BW, Moore SK, Chen Y, Furenlid LR. Maximum-Likelihood Methods for Processing Signals From Gamma-Ray Detectors. IEEE Trans Nucl Sci. 2009; 56:725–735. [PubMed: 20107527]
12. Meng LJ, Fu G. Investigation of the intrinsic spatial resolution of an intensified EMCCD scintillation camera. IEEE Trans Nucl Sci. 2008; 55:2508–2517.
13. Miller BW, Barrett HH, Furenlid LR, Barber HB, Hunter RJ. Recent advances in BazookaSPECT: Real-time data processing and the development of a gamma-ray microscope. Nuclear Instruments & Methods in Physics Research A. 2008; 591:272–275.
14. Korevaar MA, Heemskerk JW, Goorden MC, Beekman FJ. Multi-scale algorithm for improved scintillation detection in a CCD-based gamma camera. Phys Med Biol. 2009; 54:831–842. [PubMed: 19141886]
15. Johnson LC, Campbell DL, Hull EL, Peterson TE. Characterization of a high-purity germanium detector for small-animal SPECT. Phys Med Biol. 2011; 56:5877. [PubMed: 21852723]
16. Metzler SD, Greer KL, Jaszczak RJ. Helical pinhole SPECT for small-animal imaging: A method for addressing sampling completeness. IEEE Trans Nucl Sci. 2003; 50:1575–1583.
17. Furenlid LR, Wilson DW, Chen YC, et al. FastSPECT II: A second-generation high-resolution dynamic SPECT imager. IEEE Trans Nucl Sci. 2004; 51:631–635. [PubMed: 20877439]
18. Nuyts J, Vunckx K, Defrise M, Vanhove C. Small animal imaging with multi-pinhole SPECT. Methods. 2009; 48:83–91. [PubMed: 19328232]

19. Qi J, Leahy RM. Iterative reconstruction techniques in emission computed tomography. Phys Med Biol. 2006; 51:R541–578. [PubMed: 16861768]

20. Defrise M, Vanhove C, Nuyts J. Perturbative refinement of the geometric calibration in pinhole SPECT. IEEE Trans Med Imaging. 2008; 27:204–214. [PubMed: 18334442]

21. Chen CL, Wang Y, Lee JJ, Tsui BM. Toward quantitative small animal pinhole SPECT: assessment of quantitation accuracy prior to image compensations. Mol Imaging Biol. 2009; 11:195–203. [PubMed: 19048346]

22. Vanhove C, Defrise M, Bossuyt A, Lahoutte T. Improved quantification in single-pinhole and multiple-pinhole SPECT using micro-CT information. Eur J Nucl Med Mol Imaging. 2009; 36:1049–1063. [PubMed: 19219431]

23. Gambhir SS, Berman DS, Ziffer J, et al. A novel high-sensitivity rapid-acquisition single-photon cardiac imaging camera. J Nucl Med. 2009; 50:635–643. [PubMed: 19339672]

24. Bocher M, Blevis I, Tsukerman L, Shrem Y, Kovalski G, Volokh L. A fast cardiac gamma camera with dynamic SPECT capabilities: design, system validation and future potential. Eur J Nucl Med Mol Imaging. 2010; 37:1887–1902. [PubMed: 20585775]

25. Hruska CB, Phillips SW, Whaley DH, Rhodes DJ, O'Connor MK. Molecular breast imaging: use of a dual-head dedicated gamma camera to detect small breast tumors. AJR Am J Roentgenol. 2008; 191:1805–1815. [PubMed: 19020253]

26. Brem RF, Michener KH, Zawistowski G. Approaches to improving breast cancer diagnosis using a high resolution, breast specific gamma camera. Phys Med. 2006; 21(1):17–19. [PubMed: 17645987]

27. Goorden MC, Rentmeester MC, Beekman FJ. Theoretical analysis of full-ring multi-pinhole brain SPECT. Phys Med Biol. 2009; 54:6593–6610. [PubMed: 19826198]

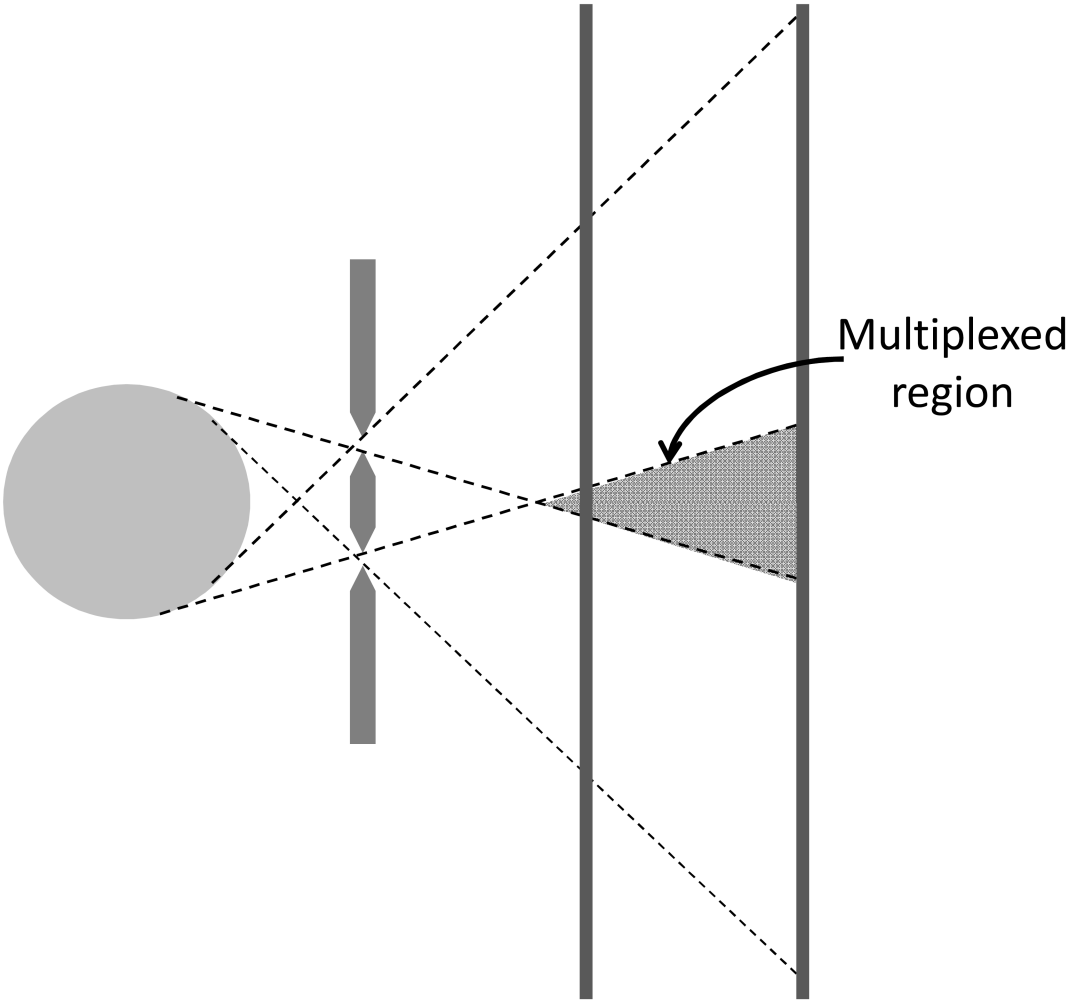

Figure 1.
In synthetic-collimator imaging, multi-pinhole projection data is acquired at multiple magnifications, with the amount of multiplexing varying with the magnification.

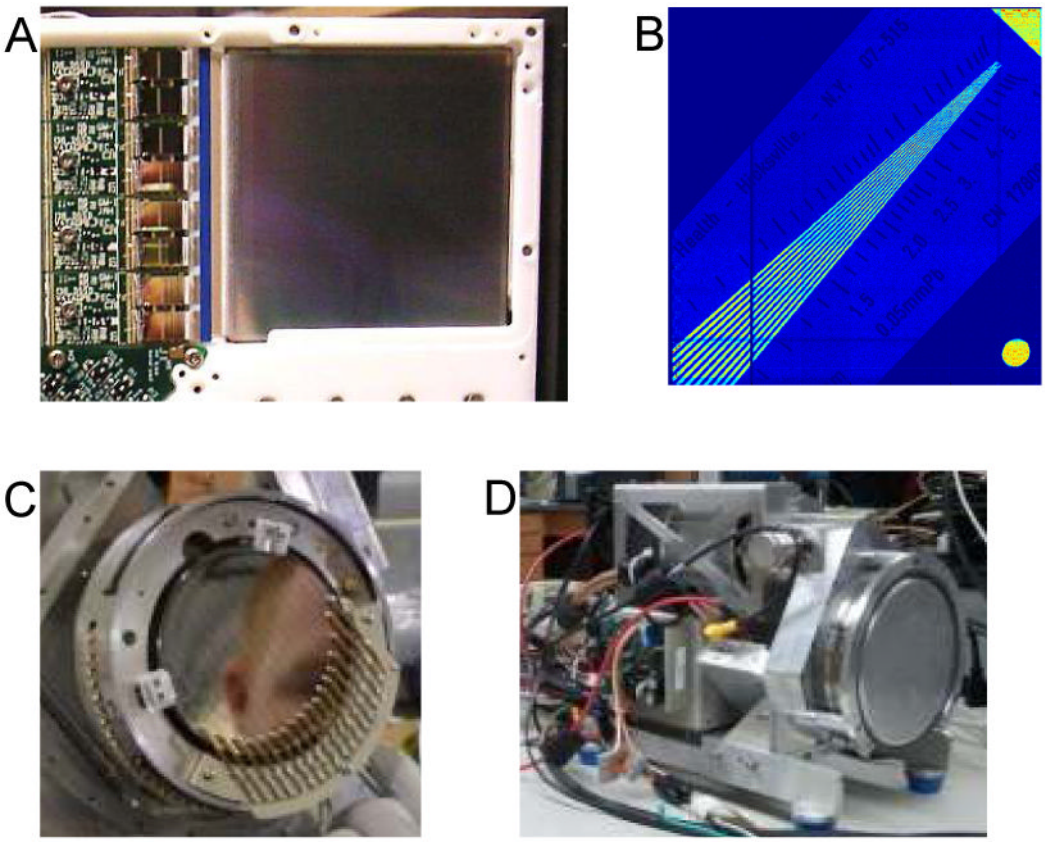

Figure 2.
(A) Photograph of a silicon double-sided strip detector in which the high-density readout electronics for one side can be seen on the left. (B) Shadow image of a radiography line-pair phantom placed in front of a silicon detector and illuminated with an Iodine-125 source. Photographs of (C) a germanium double-sided strip detector and (D) the entire detector system including readout electronics and mechanical cooling system.

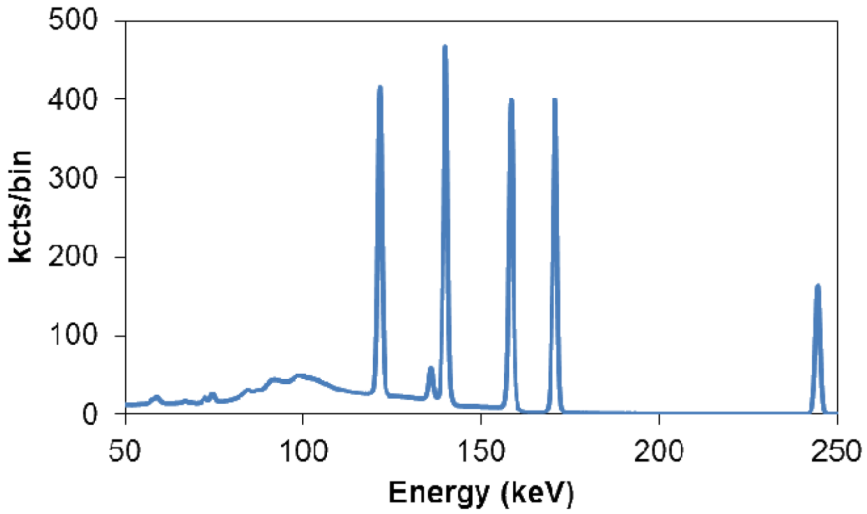

Figure 3.
Germanium pulse-height spectrum when simultaneously exposed to Cobalt-57 (122 keV and 136 keV), Technetium-99m (140 keV), Iodine-123 (159 keV), and Indium-111 (171 keV and 245 keV).